

Alpha Storage Regime in High Temperature Sub-Ignited D-T Tokamaks

S. J. Zweben, H. P. Furth, D. R. Mikkelsen, M. H. Redi, and J. N. Strachan

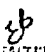
Princeton Plasma Physics Laboratory
Princeton, New Jersey 08543

Abstract

Alpha particle parameters in sub-ignited D-T tokamaks like TFTR can be optimized in a high temperature "alpha storage regime" in which the alpha particle thermalization time τ_α is long (≈ 1.0 sec) and in which the alpha particle source rate S_α is enhanced due to beam-target and beam-beam reactions (by a factor of $\approx 2-3$). Near reactor-level alpha instability parameters $\beta_\alpha(0) \approx n_\alpha(0)/n_e(0) \approx 1\%$ are predicted by simulation codes when $Q \approx 0.5-1$, while present TFTR "supershots" already have $\beta_\alpha(0) \approx n_\alpha(0)/n_e(0) \approx 0.1-0.2\%$. Plasmas in this regime can be used to test theories of collective alpha instabilities for the first time, and can also be used to provide a strong (but transient) alpha heating pulse. An experimental scenario to exploit this regime is described.

DISCLAIMER

This report was prepared as an account of work sponsored by an agency of the United States Government. Neither the United States Government nor any agency thereof, nor any of their employees, makes any warranty, express or implied, or assumes any legal liability or responsibility for the accuracy, completeness, or usefulness of any information, apparatus, product, or process disclosed, or represents that its use would not infringe privately owned rights. Reference herein to any specific commercial product, process, or service by trade name, trademark, manufacturer, or otherwise does not necessarily constitute or imply its endorsement, recommendation, or favoring by the United States Government or any agency thereof. The views and opinions of authors expressed herein do not necessarily state or reflect those of the United States Government or any agency thereof.

DISTRIBUTION OF THIS DOCUMENT IS UNLIMITED 

1. Introduction

This paper describes how sub-ignited D-T-fueled tokamaks like TFTR or JET can be used to study reactor-relevant alpha particle physics. This physics is important for future ignited plasmas since it could affect the alpha heating efficiency, the plasma confinement, or the plasma beta limits.

Most of this new physics concerns the influence of the high energy alpha particle component on plasma instabilities, and so involves dimensionless parameters such as n_{α}/n_e and β_{α} . These parameters depend on the product of the alpha source rate S_{α} and the alpha thermalization time τ_{α} , and so are only indirectly related to the thermal plasma confinement time and energy balance parameters like Q (fusion power, multiplication factor) or the ignition margin.

Since $S_{\alpha} \propto P_{\text{heat}} Q$ and $\tau_{\alpha} \propto T_e/n_e$ (see Sec. 3.1), the local alpha density scales roughly as $n_{\alpha} \propto P_{\text{heat}} Q T_e/n_e$, and so the alpha instability parameters tend to be maximized in high temperature, low density plasmas like the TFTR "supershots" [1], in which both S_{α} and τ_{α} tend to be high. Therefore, if the alpha particles are confined classically, then τ_{α} can be very long ($\tau_{\alpha} \approx 1 \text{ sec} \gg \tau_E$), allowing reactor-level alpha populations to be obtained even in sub-ignited $Q \approx 1$ machines like TFTR and JET.

The other main aspect of reactor-relevant alpha physics concerns the effect of alpha heating on the plasma. Although the average alpha heating (over space and time) is only $\langle P_{\alpha}/P_{\text{heat}} \rangle \approx 0.2$ at $Q \approx 1$, we show how plasmas with $\langle P_{\alpha}/P_{\text{heat}} \rangle \approx 0.5$ and $P_{\alpha}(0)/P_{\text{heat}}(0) \approx 0.8$ can be transiently produced by thermalizing the stored alphas after auxiliary heating is turned off.

We will call this high τ_{α} mode of operation the "alpha storage regime," where this term is intended to include the alpha "storing" phase during auxiliary heating, the alpha "coasting" phase just after auxiliary heating, and the transient alpha "heating" phase. The "storage" aspect refers to the very long expected confinement time of alphas (which is

somewhat analogous to an electron storage ring).

This paper describes various estimates and simulations for this regime, with particular application to TFTR. A brief summary of the alpha physics issues is in Sec. 2. Simplified analytic estimates of expected alpha parameters are in Sec. 3. More self-consistent code calculations for TFTR are in Sec. 4. The present capabilities of TFTR with respect to these parameters are described in Sec. 5, and the Conclusion is in Sec. 6.

2. Alpha Physics Issues

A summary of alpha instabilities and their possible effects is shown in Table 1, which is adapted from recent reviews [2]. For the purpose of this table these instabilities are ordered in terms of their frequency, which ranges from $\approx 10^1$ - 10^9 Hz for TFTR.

Note that the instabilities in Table 1 are all "collective" alpha effects, which means that the free energy of the D-T-generated high energy alpha particle population either creates or modifies these instabilities. In addition to these D-T collective effects, alpha particles can also be influenced as "single particles" by toroidal field ripple or by plasma instabilities which are not modified by alphas. However, single-particle physics is not discussed here since most experiments on these effects can be done with D-D or D- ^3He discharges [3].

At present it is not easy to assess the eventual importance of these instabilities for ignited plasmas, partly because the theories are incomplete, but mostly because experimental conditions under which they might be observed have yet to be created. The main purpose of this paper is to show that at least some of this new physics might be tested in present sub-ignited devices.

The basic parameters used to characterize collective alpha effects are n_α/n_e , β_α , V_α/V_A (the alpha speed relative to the Alfvén speed), and in one case $P_\alpha(0)/P_{\text{loss}}(0)$. These are the parameters which will be calculated in Secs. 3-5. Here we briefly summarize the main physics of these phenomena.

The very-low-frequency alpha-driven (or modified) sawtooth mode is the only one of these instabilities which depends on P_α (through the reheating process). In general, the positive feedback between increased central temperature and increased central heating may cause large sawteeth in the thermonuclear regime [2]. However, if τ_α is longer than typical sawtooth periods, the feedback effect should be relatively weak (as might be the case in TFTR or JET). One interesting physics issue which might be observed on sub-ignited plasmas is the rapid expulsion of alpha particles from inside to outside $q=1$ during sawtooth crashes [4]. Stabilization of sawteeth by alphas is also possible at high β_α [5].

Alpha-driven fishbones involve a resonance between the precession frequency of trapped alphas and the internal $m=1$ mode. White has predicted that roughly $\beta_\alpha(0) \approx 1\%$ (with $\beta_{pol}(0) > 0.3$) is necessary for this instability [6]. In analogy to neutral-beam-injection (NBI)-driven fishbones, excitation of large MHD waves and expulsion of banana-trapped alphas might be expected; however, the instability frequency would be ≈ 10 times higher for alpha-driven compared to NBI-driven fishbones.

Alpha-modified drift waves and/or ballooning modes involve the resonance between alphas and preexisting electrostatic drift or magnetic ballooning modes. Modification of these modes by alphas is potentially important since they are thought to determine tokamak transport and beta limits. The influence of alphas on stability increases with β_α and the background β_{th} . Existing calculations of such effects for TFTR [7,8] indicate that alphas decrease the threshold for ballooning instability (i.e., lower the theoretical beta limit) by $>15\%$, but do not significantly affect the drift-wave-induced transport.

Alpha-driven Alfvén waves are the most unfamiliar of these instabilities. Their growth requires that energetic particle speeds be greater than the Alfvén speed, a condition that is ordinarily not met by ions created by auxiliary heating but is met by alphas in TFTR. In general these instabilities can increase alpha transport, decrease the alpha thermalization time (which may be beneficial if the energy is transferred to background ions), or possibly increase the background plasma transport (through the wave's fields).

Table 1 shows three different types of destabilization effects for Alfvén waves. An alpha pressure gradient[9] can create low-m global Alfvén eigenmodes in plasmas similar to TFTR, although the instability threshold depends sensitively on the alpha pressure gradient and average alpha energy. An alpha loss cone [10] created by toroidal field or MHD-induced ripple can potentially create waves which (quasilinearly) limit the confined alpha population to $n_{\alpha}/n_e \approx 10^{-4}$. An alpha population inversion[11] caused by a fast turn-on of the alpha source can also create waves which increase alpha transport.

Alpha heating physics mainly concerns the slow readjustment of the plasma temperature and current profiles to the new alpha heating source function [2]. Classical alpha heating will mainly be central electron heating, so in some sense should be similar to ohmic heating. Alpha heating will also depend on the confinement of high energy alphas, so in this sense should be similar to NBI or ICRF heating. The plasma energy confinement time with alpha heating should depend on the plasma instabilities as usual, except perhaps for new alpha instability effects.

These general expectations about alpha heating can be tested to some extent on sub-ignition machines using a strong (but transient) alpha heating pulse, as described below. However, the slow profile changes produced by a dominant alpha heating source cannot be simulated in short-pulse sub-ignition machines.

3. Alpha Storage Regime

An "alpha storage regime" discharge would consist of three distinct time periods, as shown schematically in Fig. 1. Note that the time scale in this figure is drawn for a typical TFTR case.

In the approximately 2-sec-long "storing" phase the alphas are created and confined in a high temperature, low density, auxiliary heated D-T plasma similar to a TFTR "supershot" (but with ≥ 1.5 MA for good alpha confinement). By the end of this storing phase n_{α} and β_{α} are maximized, so that any alpha effects on sawteeth, fishbones, ballooning

modes, or Alfvén waves should be most apparent.

In the approximately 1-sec-long "coasting" phase just after auxiliary heating ends, the stored alpha energy decreases slowly while the plasma reestablishes a low density ohmic equilibrium. During this phase n_α/n_e and β_α/β_{th} are maximized, so that any alpha instabilities which persist at relatively low β_{th} can be studied in the absence of neutral beam ions. In this phase the stored alpha energy content can also be measured with alpha and possibly with magnetic diagnostics and compared to the expected classical alpha storage.

In the final ≈ 200 -msec-long alpha "heating" phase the remaining stored alpha energy is transferred to the background plasma by suddenly decreasing the classical alpha thermalization time. This can be done by increasing the plasma density as shown (or possibly by decreasing the temperature using impurity injection). In this phase a dominantly alpha-heated plasma is produced, but only for a short time.

In this section the expected alpha parameters for these three phases are estimated using assumed temperatures and densities, while more self-consistent computer calculations for TFTR are described in Sec. 4. Note that the simplified estimates below assume perfect alpha confinement, which may not occur if the plasma current is too low, if the toroidal field ripple is too high, or if instabilities cause anomalous alpha transport.

3.1 n_α/n_e and β_α/β_{th} in Alpha Storing Phase

Here we show, using a simple local steady-state model applicable to the end of the alpha storing phase, that these two alpha instability parameters depend mainly on the plasma temperature and not simply on the fusion power gain Q [12]. The thermonuclear reaction rate for producing alphas is (in the range $T_i \approx 20$ keV):

$$S_\alpha \approx C_1 n_D n_T T_i^{1.5} \quad (1)$$

where $C_1 \approx 1.5 \times 10^{-16} \text{ cm}^3 \text{ sec}^{-1}$ when T_i is in units of 10 keV [13]. The resulting local steady-state alpha populations (assuming perfect alpha confinement) are:

$$n_\alpha = S_\alpha \tau_\alpha \quad (2)$$

where S_α is the local D-T reaction rate, and $\tau_\alpha \approx C_2 T_e / n_e$ is the alpha thermalization time [14], where $C_2 \approx 4.5 \times 10^{13} \text{ cm}^{-3} \text{ sec}$ at $T_e \approx 10 \text{ keV}$. Note that this τ_α has a slightly weaker temperature dependence than the $T_e^{3/2}$ dependence of the alpha slowing-down time on electrons only [15]. Thus:

$$n_\alpha / n_e \approx C_1 C_2 (n_D n_T / n_e^2) T_i^{1.5} T_e \quad (3)$$

Now if alphas are also produced by non-thermonuclear (beam-target and beam-beam) reactions, where Ω = total reaction rate/thermonuclear reaction rate, then:

$$n_\alpha / n_e \approx C_1 C_2 (n_D n_T / n_e^2) T_i^{1.5} T_e \Omega \quad (4)$$

Therefore, the relative alpha population depends mainly on the plasma temperature, and not directly on the fusion power multiplication factor Q or the ignition margin. Thus, for possible TFTR D-T central parameters (see Sec. 4), $T_i(0) \approx 25\text{-}30 \text{ keV}$, $T_e(0) \approx 10\text{-}12 \text{ keV}$, $n_e(0) \approx 7\text{-}10 \times 10^{13} \text{ cm}^{-3}$, and $\Omega(0) \approx 2.5$, the central $n_\alpha(0)/n_e(0)$ is comparable to that of an ignited reactor-grade plasma at $T_i(0) = T_e(0) = 20 \text{ keV}$ and $\Omega(0) = 1$, assuming that the fuel dilution factor ($n_D n_T / n_e^2$) is the same for both.

Similarly, the relative alpha beta is:

$$\beta_\alpha / \beta_{th} = 2/3 n_\alpha \langle E_\alpha \rangle / [n_e (T_i + T_e)] \approx (n_\alpha / n_e) / (T_i + T_e) \quad (5)$$

where the average alpha energy $\langle E_\alpha \rangle \approx 1.3$ MeV is only weakly dependent on temperature or density [16]. Thus the relative alpha beta for TFTR is again comparable to that of a reactor-level ignited plasma, given the parameters above.

These formulas can be used to estimate alpha parameters for the central region of a high temperature TFTR D-T plasma at the end of the alpha storing phase of Fig. 1. We get from (4), near $T_i \approx 20$ keV and $T_e \approx 10$ keV:

$$n_\alpha/n_e \approx 0.7\% (n_D n_T/n_e^2) (T_i/10 \text{ keV})^{1.5} (T_e/10 \text{ keV}) \Omega . \quad (6)$$

Thus, for the possible TFTR central parameters cited above, assuming a possible fuel dilution factor $n_D \approx n_T \approx 0.35 n_e$ (i.e., $n_D n_T/n_e^2 \approx 0.12$), we find $n_\alpha(0)/n_e(0) \approx 1\%$. Note that for this case the alpha thermalization time is $\tau_\alpha(0) \approx 0.6$ sec, so that a typical TFTR alpha storing time of ≈ 2 sec is sufficient for the alpha population to reach this steady-state value.

Using $\langle E_\alpha \rangle \approx 1.3$ MeV we get from (5):

$$\beta_\alpha/\beta_{th} \approx (n_\alpha/n_e) 90/([T_e+T_i]/10 \text{ keV}) . \quad (7)$$

Thus, for the possible TFTR central parameters cited above, we get $\beta_\alpha(0)/\beta_{th}(0) \approx 0.2$, so at $B = 52$ kG we have $\beta_{th}(0) \approx 5\%$ and $\beta_\alpha(0) \approx 1\%$.

Alternative global scaling forms for these alpha parameters follow directly from the definitions of τ_α and S_α :

$$n_\alpha/n_e \propto P_{heat} Q T_e/(n_e^2 \times \text{plasma volume}) , \quad (8)$$

$$\beta_\alpha \propto P_{heat} Q T_e/(n_e \times \text{plasma volume} \times B^2) . \quad (9)$$

Evaluation of the central alpha parameters for TFTR using these forms requires knowledge of the alpha source radial profile. A typical "supershot" neutron source profile has $S_{\alpha}(0)/\langle S_{\alpha} \rangle \approx 7-11$, corresponding to $S_{\alpha}(0)/\langle S_{\alpha} \rangle = (1-[r/a]^2)^{\delta}$ where $\delta \approx 6-10$. Thus, with $Q \approx 0.5$, $P_{\text{heat}} \approx 30$ MW and central TFTR parameters as above (i.e., $\tau_{\alpha}(0) \approx 0.6$ sec), we get $n_{\alpha}(0)/n_e(0) \approx \beta_{\alpha}(0) \approx 1-1.5\%$, in rough agreement with the local estimates above.

3.2 Coasting Phase

After auxiliary heating is turned off, the stored alpha population decays over a thermalization time $\approx \tau_{\alpha}$ in a plasma which returns to a low density ohmic equilibrium over $\approx 2\tau_E$ ($\approx 2\tau_p$), mainly through a decrease in density as shown schematically in Fig. 1. If $\tau_{\alpha} \gg \tau_E$ during this phase, then the alpha parameters n_{α}/n_e and $\beta_{\alpha}/\beta_{\text{th}}$ will increase compared to the end of the storing phase due to these decreases in n_e and β_{th} , typically by factors of 2-3. Time-dependent simulations of the coasting phase for TFTR are described in Sec. 4.3.

3.3 Alpha Heating Phase

Alpha heating at the end of the storing phase is limited globally to $\langle P_{\alpha}/P_{\text{heat}} \rangle \approx 0.2 Q$, i.e., typically 20% for $Q \approx 1$. Such heating should be a measurable but not a dominant effect in TFTR or JET. This alpha heating is normally concentrated in the center of the plasma [17], where:

$$P_{\alpha}(0) = S_{\alpha}(0) E_{\alpha} = C_1 n_D(0) n_T(0) T_i^{1.5}(0) E_{\alpha} \Omega(0) \quad (10)$$

$$\text{and} \quad P_{\text{loss}} = [1.5[(n_D(0) + n_T(0)) T_i(0) + n_e(0) T_e(0)]] / \tau_E(0)$$

where $E_\alpha = 3.5$ MeV. Typically, $P_\alpha(0)/P_{\text{loss}}(0) \approx 0.3-0.4$ for $Q \approx 1$ plasmas (see Sec. 4.2). This level of central alpha heating is probably measurable, but again not at the reactor-relevant level $P_\alpha(0)/P_{\text{heat}}(0) \approx P_\alpha(0)/P_{\text{loss}}(0) \approx 1$.

One way to further increase alpha heating at $Q \approx 1$ is to concentrate it in time by using previously stored alpha energy to supply a transient alpha heating pulse after auxiliary heating is turned off, as shown schematically in Fig. 1. Here we estimate the maximum available $P_\alpha(0)/P_{\text{heat}}(0)$ and $\langle P_\alpha/P_{\text{heat}} \rangle$ for such a heating pulse.

To obtain a large alpha heating pulse in the way indicated schematically in Fig. 1, several time scales must be considered. First, the beam heating power should decay before the alpha heating phase begins. This happens automatically since the thermalization time for ≈ 100 keV deuterium beam ions is $\tau_b \approx 0.3 \tau_\alpha$ [4]. Next, the alpha thermalization time just after beam injection should be longer than the plasma energy confinement time after beam injection, in order to allow the plasma to reestablish an ohmic equilibrium before the alpha heating begins (to simplify the alpha heating analysis). This is possible if the density is allowed to decay rapidly after beam turn-off, since $\tau_\alpha \geq 1$ sec while $\tau_E \approx 200-300$ msec in low density ohmic TFTR discharges [18]. Lastly, the time scale for alpha thermalization after redensification τ_α^* should be as small as possible to obtain the maximum alpha heating effect, but large enough to avoid complicated profile changes, i.e., $\tau_\alpha^* \approx 100-300$ msec. This time scale determines the required density rise (or, the available density rise rate determines this time scale).

Assuming that all these time scales are optimized, we can estimate the local and global alpha heating parameters in this scenario. For the local central TFTR parameters used above we had $n_\alpha(0) \approx 10^{12}$ cm^{-3} and $\langle E_\alpha \rangle \approx 1.3$ MeV. Thus, if half (see Sec. 4.4) the stored alpha energy is retained until being rethermalized over $\tau_\alpha^* \approx 200$ msec during the alpha heating phase, we have:

$$P_{\alpha}(0) \approx n_{\alpha}(0) \langle E_{\alpha} \rangle / \tau_{\alpha}^{*} \approx 1 \text{ watt/cm}^3 \quad (11)$$

locally. Since the central ohmic heating power in TFTR for $q(0) \approx 1$ and $I \approx 2 \text{ MA}$ is $P_{\text{heat}} \approx 0.2 \text{ watts/cm}^3$, we have roughly:

$$P_{\alpha}(0)/P_{\text{heat}}(0) \approx 0.8 \quad (12)$$

at the center during this transient alpha heating phase, i.e., alpha heating is dominant locally.

The global alpha heating can be related to the total stored alpha energy just before redensification, W_{α}^{*} , which in turn is related to the the total stored alpha energy W_{α} at the end of the alpha storing phase. W_{α} can be related to Q through an average alpha thermalization time:

$$W_{\alpha} \approx 0.2 Q P_{\text{heat}} \langle \tau_{\alpha} \rangle [\langle E_{\alpha} \rangle / 3.5 \text{ MeV}] . \quad (13)$$

For TFTR $Q \approx 1$, $P_{\text{heat}} \approx 30 \text{ MW}$, $\langle \tau_{\alpha} \rangle \approx 0.5 \text{ sec}$, and $\langle E_{\alpha} \rangle \approx 1.3 \text{ MeV}$ so we have $W_{\alpha} \approx 1 \text{ MJ}$. If half of this energy remains to be thermalized by redensification over $\tau_{\alpha}^{*} \approx 200 \text{ msec}$ (as assumed above), we obtain $\langle P_{\alpha} \rangle \approx 2.5 \text{ MW}$, while $\langle P_{\text{ohmic}} \rangle \approx 2 \text{ MW}$, so that:

$$\langle P_{\alpha} / P_{\text{heat}} \rangle \approx 0.5 . \quad (14)$$

Therefore, global alpha heating is relatively much larger than in the beam-heated alpha storing phase.

The effect of this alpha heating should be to raise the stored energy of the thermal background plasma W_{th} at the expense of the stored alpha energy. Since for typical low-density ohmically heated plasma $W_{\text{th}} \lesssim 0.5 \text{ MJ}$ [18], the increase due to the above W_{α}^{*} should ideally more than double the thermal stored energy.

The following section describe simulations of these scenarios for TFTR.

4. Alpha Storage Simulation Results for TFTR

Two different plasma simulation codes were used to calculate the alpha particle parameters expected for full-power TFTR D-T plasmas. In Sec. 4.1 are the results from a relatively simple time-independent code, SURVEY, which was used to calculate alpha parameters for the steady-state "storing" phase. In Secs. 4.2-4.4 are results from a time-dependent code, BALDUR, which created detailed simulations for all three phases of a few TFTR scenarios. In general, the results of these two codes are consistent with each other and with the simplified estimates in Sec. 3.

4.1 SURVEY Simulation Results

This time-independent code was developed to survey the parameter space \bar{n}_e vs. τ_E to find regimes of $Q \approx 1$. The code assumes density and temperature profile shapes and calculates the temperatures, Q 's, and other parameters vs. \bar{n}_e from an assumed τ_E and input power. Several realistic features are taken into account [19], such as the input power profile, fuel density dilution due to beam and impurity ions, beam-target and beam-beam reactions, electron-ion coupling, and alpha particle heating.

Typical alpha particle results from this code are shown vs. \bar{n}_e in Figs. 2 and 3. In these examples the input plasma density and temperature profile shapes were taken from a TFTR supershot which had a density profile peaking factor $n_e(0)/\bar{n}_e = 2.3$, while the input power was 27 MW of NBI (50% in D and 50% in T), and $Z = 1.5$ (from carbon) was assumed (compared to $Z_{eff} \approx 3$ for present TFTR supershots).

The basic result as shown in Fig. 2 was that for a fixed τ_E the

central alpha instability parameters increase rapidly with decreasing \bar{n}_e , reaching $n_\alpha(0)/n_e(0) \approx \beta_\alpha(0) \approx 1\%$ at $\bar{n}_e \approx 4.5 \times 10^{13} \text{ cm}^{-3}$ (i.e., $n_e(0) \approx 10^{14} \text{ cm}^{-3}$) for $\tau_E \approx 0.2 \text{ sec}$ and $Q \approx 0.75$. This trend is mainly due to the increasing temperature at low density implicit in the assumption that τ_E is independent of density, which causes the alpha thermalization time τ_α to increase rapidly at low \bar{n}_e . The increased alpha population at low density is also partly caused by the increased Q due to beam-target and beam-beam reactions, as expressed in Eq. (4) or as seen in the plots of Q vs. \bar{n}_e in Fig. 2.

Also shown in Fig. 2 is the central $P_\alpha(0)/P_{\text{heat}}(0)$ vs. \bar{n}_e , which peaks at higher density than the other two alpha parameters. This variation is mainly due to decreased central NBI heating power at higher density and not to increased central alpha heating power. A central $P_\alpha(0)/P_{\text{heat}}(0) \approx 0.3-0.4$ can be obtained in steady state due to the spatial concentration of alpha heating.

Figure 3 shows the radial profiles of alpha parameters and other relevant quantities for a typical case with $Q \approx 0.5$, $\tau_E \approx 0.15 \text{ sec}$, and $\bar{n}_e \approx 4.5 \times 10^{13} \text{ cm}^{-3}$. The alpha density and beta are strongly centrally peaked, as expected, with $\delta \approx 7$ (in the notation of Sec. 3.1).

The general conclusion from this code is that operation at the lowest possible density maximizes the alpha instability parameters n_α/n_e and β_α , given the usual trend that τ_E is independent of density in strongly heated plasmas [18].

4.2 BALDUR Results for Alpha Storing Phase

The 1-D time-dependent code BALDUR [20] was used to simulate several different alpha storage scenarios in more detail than was possible with the SURVEY code. BALDUR calculates the density and temperature profiles self-consistently, given the auxiliary heating power, recycling coefficient, assumed forms for the electron and ion

heat and particle transport coefficients, etc. BALDUR also includes a finite-banana width classical alpha confinement (without ripple losses) and a classical slowing-down model in calculating alpha particle densities and heating.

Typical results for the steady-state alpha storing phase at the end of a 2-sec-long auxiliary heating pulse are shown in columns A and B of Table 2. Of course, since these transport coefficients and Z_{eff} are not yet known for anticipated $Q \approx 1$ conditions, these simulations should be considered as idealized rather than realistic predictions of TFTR D-T performance.

Column A of Table 2 shows results for a nearly optimal TFTR D-T alpha "storing" plasma with high power (30 MW of NBI), very low density ($n_e(0) \approx 7 \times 10^{13} \text{ cm}^{-3}$), relatively good confinement time ($\tau_E \approx 0.19$ sec), moderate Q (0.47), high current (3 MA), and a low $Z_{\text{eff}} = 1.3$. The result of this simulation was $T_e(0) \approx 12$ keV, $T_i(0) \approx 28$ keV, $n_D(0)n_T(0)/n_e^2(0) = 0.11$ (with $n_{\text{beam}}(0)/n_e(0) \approx 0.3$), and $Q(0) \approx 2.5$, with central alpha parameters $n_\alpha(0)/n_e(0) = 1\%$, $\beta_\alpha(0) \approx 1\%$, $\beta_\alpha(0)/\beta_{\text{th}}(0) = 0.3$, and $P_\alpha(0)/P_{\text{loss}}(0) \approx 0.1$.

These results can be compared to the simplified estimates given in Sec. 3. Application of Eqs. (6) and (7) using BALDUR's central parameters gives $n_\alpha(0)/n_e(0) = 1\%$ and $\beta_\alpha(0)/\beta_{\text{th}}(0) = 0.25$, which agrees with BALDUR's estimates to well within a factor of 2. The central alpha heating parameter $P_\alpha(0)/P_{\text{loss}}(0)$ as calculated through the simplified estimate of Eq. (8) also agrees to within a factor of 2 of BALDUR's estimate of $P_\alpha(0)/P_{\text{loss}}(0) \approx 0.1$. The global alpha heating was $\langle P_\alpha/P_{\text{loss}} \rangle \approx 0.1$ as expected for $Q \approx 0.5$.

Column B of Table 1 gives the results of a similar BALDUR run but with 7.5 MW of central ICRF heating added. The central temperatures increase by about 40% and the central $n_\alpha(0)/n_e(0)$ and $\beta_\alpha(0)$ increase by about 50%. This example shows that central plasma heating, when accomplished without fueling, is very effective in increasing the central alpha parameters if, as assumed here, the plasma confinement does not

degrade substantially with added power.

The predicted $n_{\alpha}(0)/n_e(0)$ and $\beta_{\alpha}(0)$ from these BALDUR simulations are also roughly consistent with the SURVEY code results for the same assumed heating power, confinement time, impurity level, and plasma density (and with a previous low density BALDUR simulation[3]). Of course, both these results depend on the degree to which the assumptions in these codes match the reality of such discharges, which have yet to be produced. More details concerning the modeling choices used in BALDUR are described in the Appendix, and comparisons with present experimental results are given in Sec. 5.

4.3 BALDUR Results for Coasting Phase

In Columns C and D of Table 1 are results for the same simulations as in A and B, respectively, but for a time 500 msec after the end of the NBI heating phase, at which time the beam ion density is negligible. It is interesting to note that the central alpha instability parameters $n_{\alpha}(0)/n_e(0)$ and $\beta_{\alpha}(0)/\beta_{th}(0)$ actually increase by a factor of 2-3 after beam turn-off, as anticipated in Sec. 3.2, mainly due to the rapid decrease of $n_e(0)$ to its pre-NBI level of $\approx 2 \times 10^{13} \text{ cm}^{-3}$ after beam fueling ceases. This coasting phase can be used to look for alpha instabilities and to check the classical modelling of alpha confinement and thermalization without the (possibly) competing effect of NBI-driven instabilities. The alpha beta during this phase may be directly measurable through the difference between the magnetic and kinetic betas.

Also interesting is the relatively high central and global alpha heating $\langle P_{\alpha}/P_{loss} \rangle \approx P_{\alpha}(0)/P_{heat}(0) \approx 0.5$ after beam turn-off, due mainly to the rapid decay of beam heating. However, even though the alpha heating in these cases is relatively strong compared to other heating sources, the decay of thermal energy after NBI still dominates the power balance at this time, such that $\langle P_{\alpha}/P_{loss} \rangle \approx P_{\alpha}(0)/P_{loss}(0) \approx 0.1$ at 500 msec after NBI. Thus the net

thermal stored energy during this phase is still decreasing despite the alpha heating (since $P_{\text{loss}} > P_{\text{heat}}$ until ohmic equilibrium is completely reestablished).

4.4 BALDUR Results for Alpha Heating Phase

In Fig. 4 are the results of a BALDUR run similar to that in column B (and D), but with a pellet injected 0.9 sec after beam turn-off to thermalize the stored alpha energy, as shown schematically in Fig. 1. The pellet was timed to be late enough so that the plasma had nearly reestablished an ohmic equilibrium, but early enough so that a significant fraction of the original stored alpha energy ($\approx 50\%$) remained in the plasma. This run used a relatively small pellet which increased \bar{n}_e from $1.2 \times 10^{13} \text{ cm}^{-3}$ to $2.2 \times 10^{13} \text{ cm}^{-3}$ (and increased the volume-averaged density $\langle n_e \rangle$ by about a factor of 2).

Just before pellet densification at 0.7 sec after NBI turn-off there is still 0.8 MJ (of the original 1.4 MJ) of alpha energy stored in this simulation, with a nearly equal amount of thermal stored energy, i.e., $\langle \beta_\alpha / \beta_{\text{th}} \rangle \approx 1$. This large ratio is possible only transiently (see Eq. 5). Also at this time $\langle P_\alpha \rangle \approx 0.85 \text{ MW}$, $\langle P_{\text{oh}} \rangle \approx 0.3 \text{ MW}$, and $\langle P_{\text{loss}} \rangle \approx 2.5 \text{ MW}$, i.e., $\langle P_\alpha / P_{\text{heat}} \rangle \approx 0.7$ and $\langle P_\alpha / P_{\text{loss}} \rangle \approx 0.3$. Near the center (inside $a/4$) $P_\alpha(0) \approx 0.3 \text{ MW}$, $P_{\text{oh}}(0) \approx 0.04 \text{ MW}$, and $P_{\text{loss}}(0) \approx 0.9 \text{ MW}$, i.e., $P_\alpha(0) / P_{\text{heat}}(0) \approx 0.9$ and $P_\alpha(0) / P_{\text{loss}}(0) \approx 0.3$. Therefore, the heating effect of alphas could be deduced only after a large correction for the time-dependent decrease of stored thermal energy.

However, starting with the pellet densification at 5.6 sec, about 50% of the the stored alpha energy is thermalized in $\approx 200 \text{ msec}$, as shown by the drop in $\langle \beta_\alpha \rangle$ in Fig. 4. Thus the average alpha heating over this time is about $\langle P_\alpha \rangle \approx 1.5 \text{ MW}$, while the average ohmic heating was about $\langle P_{\text{oh}} \rangle \approx 0.7 \text{ MW}$. As a result of this heating the average thermal stored energy $\langle \beta_{\text{th}} \rangle$ increases by about 25% above the value it would

have had with pellet injection but without alpha heating. This increase in global thermal energy content due to alpha heating could be measured by the standard thermal plasma kinetic and/or magnetic diagnostics.

The central alpha heating rate was determined by the pellet density deposition profile, which in this case was peaked at about $r/a \approx 0.1$ (through use of an unrealistically high pellet speed for this size pellet). During the strong alpha heating phase the central (inside $a/4$) heating power is $P_\alpha(0) \approx 0.3$ watt/cm² with $P_\alpha(0)/P_{\text{heat}}(0) \approx 0.8$, i.e., similar to the simple estimates of Eqs. (11) and (12). However, local alpha heating effects might be difficult to isolate, since the temperature profile is still reequilibrating itself in response to the pellet.

Another run was made with a larger pellet in which $\langle n_e \rangle$ was increased by a factor of 5 instead of 2 in an attempt to increase the alpha heating pulse. In that case the average alpha heating over 200 msec was increased from ≈ 1.5 MW in the previous run to ≈ 3 MW, and the increase in thermal stored energy at 5.8 sec was about 50% instead of 25%. On the other hand, the large changes in $\langle T \rangle$ and $\langle n_e \rangle$ and their profiles which would be induced by the pellet would make interpretation of alpha heating effects difficult. Perhaps the use of a more gentle neutral gas "puff" rather than a pellet would be more appropriate.

5. Present TFTR Capabilities

Access to this new alpha physics depends on actual plasma performance. In this section we estimate the alpha particle parameters which would be obtained if presently existing TFTR plasmas were run with D-T fuel. The fueling is assumed to be from a 50%/50% mixture of nominal 120 keV deuterium and tritium neutral beams.

The present TFTR central alpha parameters can be estimated in several different ways. One way, through Eqs. (6) and (7), uses the local central temperatures, the central Ω , and the central fuel ion depletion factor. For the best documented "supershot"[1] we have D-D central parameters of $T_i(0) \approx 22$ keV, $T_e(0) \approx 7.5$ keV (after recalibration),

$n_e(0) \approx 6.5 \times 10^{13} \text{ cm}^{-3}$, $n_d(0)/n_e(0) \approx 0.5$ (with $Z_{\text{eff}} \approx 3$ and $n_{\text{beam}}(0)/n_e(0) \approx 0.15$), and global parameters $\Omega \approx 4$, $B = 5.2 \text{ T}$, and $I = 1 \text{ MA}$. Assuming $\Omega(0)$ is the same as the global Ω (which is reasonable since most of the fusion reactions come from the center), we find using $(n_D n_T / n_e^2) = 0.062$ that $n_\alpha(0)/n_e(0) \approx 0.3\%$ and $\beta_\alpha(0) \approx 0.3\%$ (both with at least $\pm 50\%$ uncertainty).

A different estimate for the same alpha parameters can be made using the global Q_{eq} and P_{heat} through Eqs. (8) and (9). For the same central TFTR parameters we get $\tau_\alpha(0) \approx 0.5 \text{ sec}$ when $P_{\text{heat}} = 15 \text{ MW}$, $Q_{\text{eq}} \approx 0.25$ (after neutron recalibration). Assuming as in Sec. 3.1 that $S_\alpha(0) / \langle S_\alpha \rangle \approx 9$ (consistent with the calculated neutron source profile for this shot), we find again that $n_\alpha(0)/n_e(0) \approx 0.3\%$ and $\beta_\alpha(0) \approx 0.3\%$ (again with at least $\pm 50\%$ uncertainty).

A third estimate was made using the SURVEY code with assumed parameters similar to the shot above, namely $T_i(0) = 26.2 \text{ keV}$, $T_e(0) = 7.8 \text{ keV}$, $n_e(0) = 6 \times 10^{13} \text{ cm}^{-3}$, $n_D n_T / n_e^2 = 0.085$, $B = 52 \text{ kG}$, $I = 0.9 \text{ MA}$, $Q = 0.22$, $P_{\text{heat}} = 13 \text{ MW}$, and $\tau_E = 0.11 \text{ sec}$. The results $n_\alpha(0)/n_e(0) \approx 0.28\%$ and $\beta_\alpha(0) \approx 0.17\%$ are again roughly consistent with the other two estimates.

Global alpha heating levels for present TFTR plasmas in the steady-state near the end of the storing phase would be $\langle P_\alpha / P_{\text{Loss}} \rangle \approx 0.05$, since $Q \approx 0.25$. Central alpha heating according to the estimate of Eq. (10) is presently $P_\alpha(0) / P_{\text{Loss}}(0) \approx 0.1$ (with $P_\alpha(0) \approx 0.2 \text{ watts/cm}^3$ and $P_{\text{Loss}}(0) \approx 2 \text{ watts/cm}^3$), which is roughly consistent with the SURVEY run for a similar plasma mentioned above.

These estimates for present TFTR results should be corrected for the imperfect neoclassical alpha confinement for present plasma currents of only $\approx 1 \text{ MA}$. The prompt-loss fraction for alphas inside $r/a = 0.3$ is $\approx 25\%$ (from a 1-MA BALDUR run), and the finite banana width of centrally-born alphas further reduces the central alpha density by $\approx 20\%$. Thus the estimates above should be divided by ≈ 2 to give the present TFTR central alpha parameter range, i.e.,

$n_{\alpha}(0)/n_e(0) \approx \beta_{\alpha}(0) \approx 0.1-0.2\%$ and $P_{\alpha}(0)/P_{\text{loss}}(0) \approx 0.05-0.1$.

It should also be noted that any additional "single particle" alpha losses such as those due to toroidal field ripple or interactions with existing instabilities will further reduce these alpha parameters. Of course, the main objective of these experiments is to determine whether any additional "collective" alpha losses also exist.

For the coasting phase the main concern is the density and temperature evolution after auxiliary heating. For the 1-MA "supershot" referred to above [1], the total stored energy fell by about a factor of 6 in 0.5 sec after NBI, while \bar{n}_e fell by about a factor of 3 and $T_e(0)$ fell by only $\approx 30\%$. In the full-power TFTR simulations of Sec. 4 the stored energy fell by a factor of 4 in 0.5 sec after NBI, while \bar{n}_e fell by a factor of 2.5 and $T_e(0)$ stayed about the same. Therefore the existing plasmas are roughly similar to the simulations with respect to the expected x2-3 increases in n_{α}/n_e and $\beta_{\alpha}/\beta_{\text{th}}$ in the coasting phase relative to the storing phase.

Recent TFTR experiments on the burnup of 1 MeV tritons have analyzed this coasting phase in some detail [21]. There it was shown that these tritons, which are created in D-D reactions during the storing phase and which should have slowing-down times and confinement properties similar to alphas, were confined for ≈ 1 sec during the coasting phase. This is very long, as expected, but still somewhat less than the simulation result of $\tau_{\alpha} \approx 2-3$ sec in this phase (Table 2) due to the lower T_e in the present experiments.

Densification of TFTR plasmas during the coasting phase has also been tried recently by injecting 3.5-mm-diameter deuterium pellets into the low-density plasmas 0.25-1.5 sec after NBI [22]. For pellet injection at 0.75 sec after NBI, \bar{n}_e increased by x10 and $n(0)$ by x7, i.e., far more than necessary to realize the simulation of Fig. 4. In this case the alpha thermalization time was reduced to $\tau_{\alpha} \approx 10$ msec near the center, and a corresponding transient increase in the triton burnup similar to transient alpha heating was observed. However, the density and temperature profiles were very distorted, and a large sawtooth-like

event was observed just after pellet injection. Thus, for practical purposes, either a much smaller pellet (which would not penetrate to the center) or gas puffing should be used for densification.

The expected increases in beam power (from ≈ 15 MW to ≈ 30 MW), plasma current (from 1 MA to 2.5 MA), and Q (from ≈ 0.25 to ≈ 0.5) should increase the alpha parameters to $n_{\alpha}(0)/n_e(0) \approx \beta_{\alpha}(0) \approx 1\%$ according to the scaling of Eqs. (8) and (9) or to the simulation results of Table 1 or Fig. 2. Even if Q cannot be increased above present levels, an increase of $\tau_{\alpha}(0)$ from ≈ 0.5 sec to ≈ 1.0 sec (e.g., by further lowering $n_e(0)$ or increasing $T_e(0)$ with additional heating) could also bring the alpha parameters into this range.

6. Conclusions

A high temperature "alpha storage regime" was described in which reactor-relevant alpha instability parameters n_{α}/n_e and β_{α} can be obtained even in the present generation of sub-ignited D-T tokamaks such as TFTR or JET. These plasmas can be used to test theoretical models of potential alpha instabilities such as alpha fishbones, alpha-modified ballooning modes, and/or alpha-driven Alfvén waves.

An experimental scenario was described to exploit this regime in TFTR. It consists of an alpha "storing" phase during auxiliary heating, an alpha "coasting" phase in which the alphas remain after the beam heating ends, and an alpha "heating" phase during which the remaining alpha energy is collisionally transferred to the background plasma. Simple estimates and computer simulations were used to find the expected alpha parameters for present and anticipated TFTR conditions.

A comparison between the resulting alpha parameters for TFTR and those expected for various ignition machines is shown in Table 3. Relative alpha densities in TFTR could be comparable to or higher than those in ignited plasmas. Alpha betas in TFTR could be higher than those in low-temperature ignition devices, and within about a factor of 2.5 of those in high-temperature ignition devices (which run at higher thermal beta than TFTR). The parameter $V_{\alpha}/V_{\text{Alfvén}}$ is lower in TFTR than in

higher density ignition devices, but still high enough for Alfvén wave instabilities. The alpha power source in TFTR is, of course, less dominant than in ignition devices, but its heating effects should be measurable both in steady-state and transient experiments.

The conclusion from this table and this paper is that TFTR can explore reactor-relevant alpha instability and confinement physics, and can be useful for a preliminary study of alpha heating physics.

Acknowledgments

We thank G. Bateman, L. Chen, R. Goldston, D. Jassby, D. Meade, D. Post, G. Rewoldt, P. Rutherford, G. Schmidt, D. Sigmar, and R. White for many helpful comments. This work was supported by the U.S. Department of Energy Contract No. DE-AC02-76-CHO3073.

APPENDIX

In this Appendix we summarize several related BALDUR runs which have been used for theoretical studies of potential alpha particle effects on TFTR. We describe how they are related to the cases shown in Table 2 and in Fig. 4. We also show how different choices of transport models can lead to similar final plasma temperatures. All of these simulations were based on a prototype simulation of a TFTR supershot [23].

The tokamak parameters for the four cases considered are given in Table 4. BALDUR run ALT020 was used by Sigmar and Spong for calculations of the destabilization of ballooning modes[8]. ALT046 was identical to ALT020 but with ICRF heating added during the beam phase and with the addition of pellet injection after the heating phase. ALT046 results are shown in Fig. 4. ALT068 of Table 2 was similar to ALT046 but with slightly increased B and I (4.5 T vs. 5 T and 2.5 MA vs. 3.0 MA), and a different model for electron thermal losses. ALT069 of Table 2 was identical to ALT068 but without the ICRF heating.

Two models for electron conduction losses were used, as shown in Table 4. Model 1 set $\chi_e = 0.38 \times 10^3 + 0.5 \times 10^3 (r/a)^3$, with no density or power dependence (ALT020 and ALT046). Model 2 used the parametric scaling with power, density, etc. of a microinstability-based model[24] for χ_e and χ_i [25] (ALG003 and ALT069).

For ALG003 the overall numerical factor used in the electron conduction losses yields a predicted electron temperature in agreement with a supershot experiment, within 12%. For ALT069 this numerical factor is not calibrated to experiment but rather adjusted to obtain $Q \approx 0.5$. The χ_e numerical factor is three times larger in ALG003 but the convective multiplier is smaller (Table 4).

In all simulations we assumed Chang-Hinton neoclassical ion conduction losses with a unity neoclassical multiplier. The η_i parameter was below 1.5 and the suppression of anomalous ion transport due to η_i modes was assumed. This assumption is consistent with simulations of

TFTR experiments [26], although recent ion temperature measurements on TFTR indicate $\chi_i \alpha \chi_e$ even for peaked density profile supershots [27].

ALG003 also differs from ALT069 in that helium ash profiles were computed and the particle modelling was somewhat different. In Fig. 5 are shown the simulated plasma density and temperature profiles as well as the q , β_α , n_α , and n_{He} profiles at beam turnoff for the case ALG003. This simulation has been used by Rewoldt [7] for studies of the high- n ballooning mode stability of TFTR.

In all these BALDUR runs the density was determined by an assumed particle diffusion coefficient which was adjusted to be very large for deuterium in order to keep the equilibrium density low. This generally resulted in significant energy losses due to convection. The D/T species mix was kept near optimum by injecting D beams into an initially pure T plasma, and artificially reducing the thermalized T diffusion coefficient relative to D (more realistic simulations would use tritium beams).

Table 5 compares the temperatures, densities, etc. for these four cases at the end of the alpha storing phase. The simulations differ primarily in that the conduction models and convective multipliers cause different losses and consequently different final electron and ion temperatures. No models for convective and conductive losses are yet standard for predictions involving auxiliary heated tokamaks; however, recent analysis of TFTR supershots [28] has found an ion convective multiplier $>5/2$ and an electron convective multiplier $>3/2$ within $r=a/3$. It is clear from Tables 4 and 5 that the choice of convective multiplier can be as important as the electron diffusivity model in obtaining high values of the fusion Q and alpha parameters.

REFERENCES

- [1] STRACHAN, J.D. et al., Phys. Rev. Lett. 58, (1987) 1004.
- [2] SIGMAR, D.J., Physica Scripta, Vol. T16, p.6 (1987); D.J. Sigmar, MIT Plasma Fusion Center Report PFC/CP-88-1, 1988. Table 1 was prepared with the help of L. Chen, G. Rewoldt, D. Sigmar, and R. White.
- [3] ZWEBEN, S., Physica Scripta, Vol. T16, (1987) 119.
- [4] MARTIN, G. et al., Physica Scripta Vol. 167 (1987) 160.
- [5] WHITE, R.B., RUTHERFORD, P.H., COLESTOCK, P., and BUSSAC, M.N., Phys. Rev. Lett. 60 (1988) 2038.
- [6] WHITE, R., Proc. Alpha Particle Effects Workshop, Courant Inst., NYU, 1985.
- [7] REWOLDT, G., Princeton Plasma Physics Laboratory Report PPPL-2532, 1988 (submitted to Phys. Fluids).
- [8] SPONG, D.A., SIGMAR, D.J., RAMOS, J.J., Fus. Tech. 13 (1988) 428.
- [9] LI, Y.M., MAHAJAN, S.M., and ROSS, D., Phys. Fluids 30 (1987) 1466.
- [10] ANDERSON, D., and LISAK, M., Phys. Fluids 27 (1984) 925.
- [11] SIGMAR, D., Proc. Int'l. School of Plasma Physics, Varenna, Italy, 1979, EUR Fu BRU/XII/476/80, p.27.
- [12] HOULBERG, W., Proc. Alpha Particle Effects Workshop, Courant Institute, N.Y.U., Dec. 1985.

- [13] SADLER, G. and VAN BELLE, P., JET-IR(87)08
- [14] JASSBY, D., Nucl. Fus. 17 (1977) 309.
- [15] POST, D., Applied Atomic Collision Physics, Vol. 2, Academic Press, p. 381, 1984.
- [16] JASSBY, D., Nucl. Fus. 15 (1975) 453.
- [17] REDI, M.H., ZWEBEN, S.J., BATEMAN, G., Fusion Technology, Vol. 13, (1988) 57.
- [18] HAWRYLUK, R. et al., Proc. 11th International Conf. on Plasma Physics and Controlled Nuclear Fusion Research, Kyoto, 1986; IAEA-CN-47 paper A-1-3.
- [19] MIKKELSEN, D.R., private communication (1988).
- [20] SINGER, C.E. et al., Comp. Physics Comm. (in press).
- [21] BARNES, C. et al., 15th European Conf. on Cont. Fusion and Plasma Heating, Dubrovnik, 1988.
- [22] MURPHY, T., et al., 15th European Conf. on Cont. Fusion and Plasma Heating, Dubrovnik, 1988.
- [23] TANG, W.M. et al., 15th European Conf. on Cont. Fusion and Plasma Heating, Dubrovnik, 1988.
- [24] TANG, W.M. et al., Proc. 11th Int'l. Conf. on Plasma Physics and Cont. Nucl. Fus. Res., Kyoto, 1986 paper IAEA-CN-47/A-VI-1-2.
- [25] TANG, W.M., Nucl. Fus. 26 (1986) 1605.
- [26] REDI, M.H. et al., Nucl. Fus. 27 (1988) 2001.

[27] FONCK, R. et al., 15th European Conf. on Controlled Fusion and Plasma Heating, Dubrovnik, 1988.

[28] ZARNSTORFF, M. et al. Proc. 15th European Conf. on Controlled Fusion and Plasma Heating, Dubrovnik, 1988.

Table 1. Collective Alpha Instabilities

INSTABILITY	TFTR FREQUENCY	PHYSICAL MECHANISM(S)	IMPORTANT PARAMETERS	POSSIBLE EFFECTS
Alpha-Driven Sawteeth	≥ 10 Hz	Central Electron heating by α 's → sawtooth crash	$\frac{P_{\alpha}(0)}{P_{\text{heat}}(0)}$	Modification of $q(r)$ profile; expulsion of α 's from center
Alpha-Driven Fishbones	$\geq 10^4$ Hz	Resonance of α precession and internal $m=1$ mode	$\beta_{\alpha}(0)$ $\beta_{\text{th}}(0)$ $\omega_{d\alpha}/\omega_A$	Expulsion of trapped alphas (1/4-1/3 of all alphas)
Alpha-Driven Drift Wave or Ballooning Modes	$\geq 10^5$ Hz	Resonance with $m \gg 1$ modes	n_{α}/n_e , β_{α} β_{th} and Gradients	Effect on beta limits; effects on plasma transport coefficients
Alpha-Driven Alfvén Waves	$\sim 10^6$ - 10^7 Hz ($\omega \ll \omega_{c\alpha}$)	$v_{\alpha} > v_A$ excites Alfvén modes	V_{α}/v_A $\omega_{+\alpha}/\omega_A$ $\nabla\beta_{\alpha}$	Anomalous alpha transport; electron heating
Alpha-Loss-Cone-Driven Alfvén Waves	$\sim 10^8$ Hz $\omega \sim \omega_{c\alpha}$	Electromagnetic ion cyclotron wave generation	TF Ripple n_{α}/n_e	Anomalous loss of both trapped and circulating α 's; ion heating
Alpha-Population-Inversion Driven Alfvén Wave	10^8 - 10^9 Hz ($\omega \sim 10 \omega_{c\alpha}$)	$\partial f_{\alpha}/\partial v > 1$ → alpha cyclotron emission	$\frac{1}{S_{\alpha}} \frac{\partial}{\partial t} (S_{\alpha} \tau_{\alpha})$	Anomalous slows alphas; emits EM waves; heats bulk ions

Symbols: $\omega_{d\alpha}$ = alpha precession frequency; ω_A = Alfvén frequency, $\omega_{c\alpha}$ alpha cyclotron frequency, $\omega_{+\alpha}$ = alpha diamagnetic frequency.

Table 2: Low-Density Alpha-Storage Mode DT Projections

	<u>STORING PHASE</u>		<u>COASTING PHASE</u>	
	<u>A</u>	<u>B</u>	<u>C</u>	<u>D</u>
Time(sec)	4.7	4.7	5.3	5.3
Q	0.47	0.38	---	---
P _{NB} (MW)	30	30	---	---
P _{RF} (MW)	0	7.5	---	---
n _e (10 ¹⁹ m ⁻³)	3.4	3.0	1.3	1.2
n _e (0) (10 ¹⁹ m ⁻³)	6.7	5.6	2.1	2.0
T _e (0)(keV)	12.0	16.4	13	15.2
T _i (0) (keV)	28.0	44.0	13	16.5
Z _{eff}	1.3	1.3	1.5	1.3
τ _E (sec)	0.19	0.19	0.28	0.21
I _p (MA)	3.0	3.0	3.0	3.0
β _{Troyon} (%)	2.2	2.2	2.2	2.2
<β _α > (%)	1.3	1.5	0.32	0.41
β _{th} (0)(%)	3.3	4.2	0.8	0.9
τ _α (0) (sec)	0.76	1.2	2.5	3.1
<β _α >(%)	0.13	0.19	0.09	0.15
β _α (0)(%)	1.0	1.4	0.65	1.0
n _α (0)/n _e (0)(%)	1.0	1.7	2.4	4.0
W _α (MJ)	0.92	1.3	0.64	1.0
P _α /P _{heating}	0.10	0.08	0.48	0.51
P _{α(a/4)} /P _{heating(a/4)}	0.11	0.05	0.66	0.67
P _α /P _{loss}	0.10	0.08	0.11	0.10
P _{α(a/4)} /P _{loss(a/4)}	0.11	0.05	0.17	0.18
Ω	2.5	2.3	---	---
Run No.	ALT69	ALT68	ALT069	ALT068

Table 3. Alpha-Particle Plasma Parameters

Parameter	TFTR Now*	TFTR Objective	"Marginal Ignition"(A)	CIT High-T(B)	ITER(C)
<u>1. Alpha-particle plasma physics</u>					
$n_{\alpha}(0)/n_e(0)$	0.1-0.2%	1%	0.1%	0.9%	0.7%
$\beta_{\alpha}(0)$	0.1-0.2%	1%	0.2%	2.5%	2.3%
$V_{\alpha}/V_{\text{Alfven}}$	1.5-2.0	1.7	2.5	2.6	2.8
<u>2. Heat flow from a fusion power source</u>					
$P_{\alpha}(0)/P_{\text{loss}}(0)$	0.05-0.1	0.4	~1	~1	~1
$\langle P_{\alpha}/P_{\text{loss}} \rangle$	0.03-0.07	0.2	0.8	~1	~1

*Best results obtained in individual TFTR deuterium-plasma supershots (e.g. #22553, #22984 [1], #26151, and #30969 [28]).

(A) $T(0) = 10 \text{ keV}$, $n(0) = 10^{15} \text{ cm}^{-3}$, $B = 125 \text{ kG}$

(B) $T(0) = 23 \text{ keV}$, $n(0) = 6 \times 10^{14} \text{ cm}^{-3}$, $B = 100 \text{ kG}$

(C) $T(0) = 20 \text{ keV}$, $n(0) = 2 \times 10^{14} \text{ cm}^{-3}$, $B = 50 \text{ kG}$

Table 4. Plasma Parameters for Alpha Storage Scenarios

	R	a	B _z	I _p	Z _{eff}	χ_e^{model}	P _{beam}	Convective Ion	Multiplier Electron
ALT020	255	82	45	2.5	1	1	25 MW	5/2	5/2
ALT 046	255	82	45	2.5	1	1	25+7(ICRF)	5/2	5/2
ALT069	260	95	50	3.0	1.3	2	30	5/2	3/2
ALG003	260	95	50	3.0	1.3	2	25	3/2	3/2

Table 5. Simulation Results for Various Alpha Storage Scenarios

	<u>ALT020</u>	<u>ALT046</u>	<u>ALT069</u>	<u>ALG003</u>
Q	0.44	0.43	0.48	0.42
P (MW)	25 (NBI)	25(NBI)+7(ICRF)	30(NBI)	25(NBI)
$n_e(\text{cm}^{-3})$	3.4×10^{13}	3.2×10^{13}	3.4	3.0
$\tau_E(\text{sec})$	0.15	0.16	0.19	0.20
$n_e(0)(\text{cm}^{-3})$	7.4×10^{13}	7.0×10^{13}	6.7	5.5
$T_e(0)(\text{keV})$	11	17	12.	9.8
$T_i(0)(\text{keV})$	25	44	28	41
$W_\alpha(\text{MJ})$	0.7	1.4	0.9	0.7
$\beta_\alpha(0)(\%)$	0.7	1.7	1.0	0.7
$n_\alpha(0)/n_e(\%)$	0.7	1.6	1.0	0.8
$\langle \beta_\alpha \rangle(\%)$	0.17	0.26	0.13	0.11
$\langle n_\alpha/n_e \rangle$	---	1	---	---
Z_{eff}	1	1	1.3	1.3

FIGURE CAPTIONS

(1) Schematic time-history of an alpha storage regime plasma, with a time scale appropriate for TFTR.

(2) SURVEY code results for steady-state alpha parameters in TFTR. The four graphs are for central (i.e., $<a/4$) β_α/β_{tot} , β_α , n_α/n_e , and P_α/P_{heat} . For each graph lines of constant τ_E (dashed) and Q (solid) are shown.

(3) SURVEY code results for radial profiles of alpha parameters for TFTR. The density and temperature profiles are fixed to be similar to TFTR supershots. The resulting alpha parameters are strongly centrally peaked, as expected. The central values for this case are $n_\alpha(0) = 5.2 \times 10^{11} \text{ cm}^{-3}$, $n_\alpha(0)/n_e(0) = 0.52\%$, $\beta_\alpha = 0.65\%$ and $\beta_\alpha(0)/\beta_{tot}(0) = 10\%$.

(4) BALDUR code results for the alpha coasting and alpha heating phases of a $Q \approx 0.5$ TFTR case. In (a) are the volume-averaged temperatures and densities. In (b) are the volume-averaged betas for alphas, beams, and the thermal plasma. In (c) are the total powers for alpha, beam, and ohmic heating and the total power loss rate.

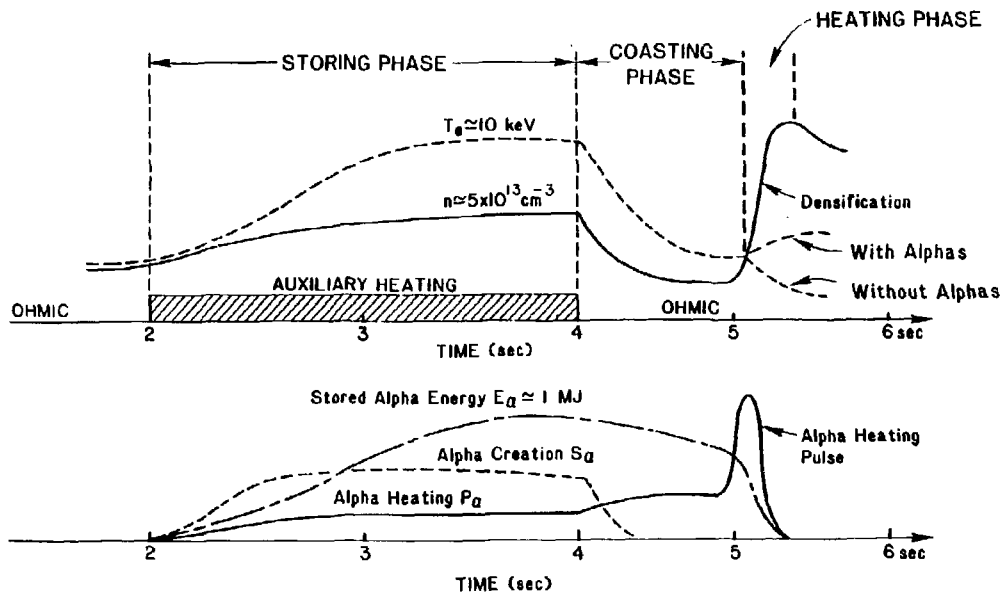


FIG. 1

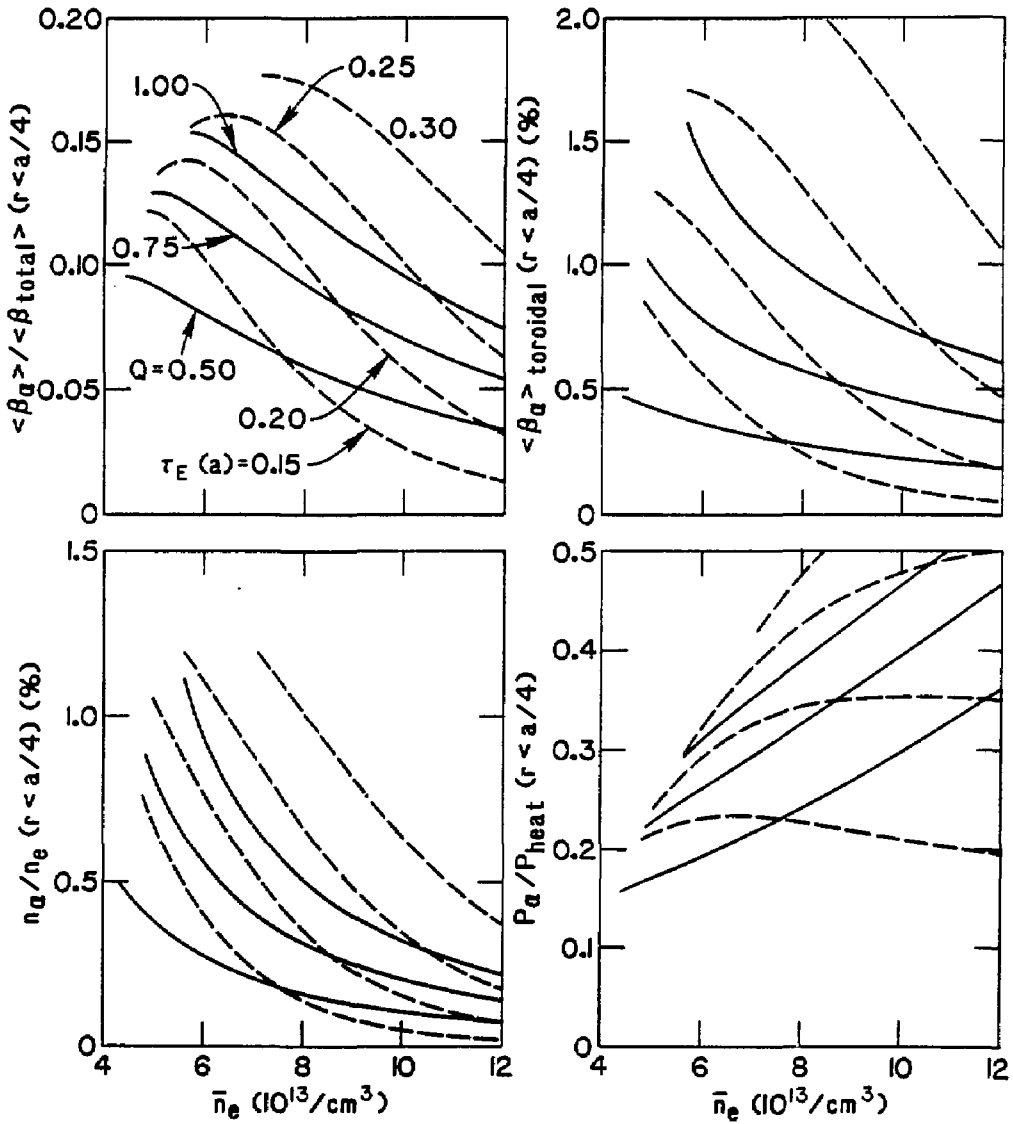


FIG. 2

#88X0567

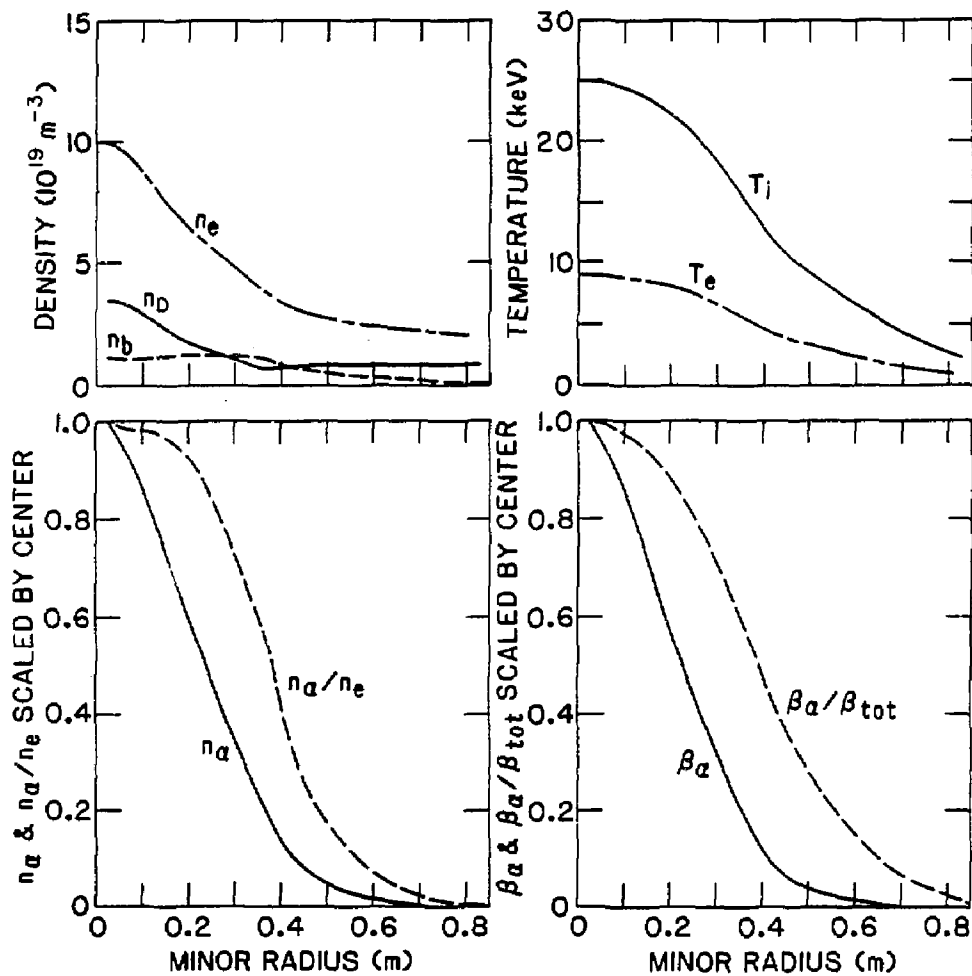


FIG. 3

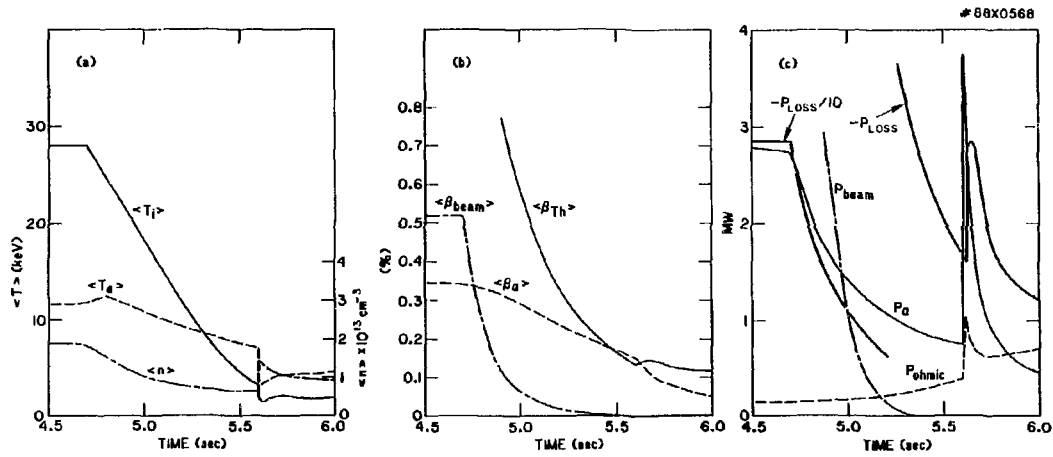


FIG. 4

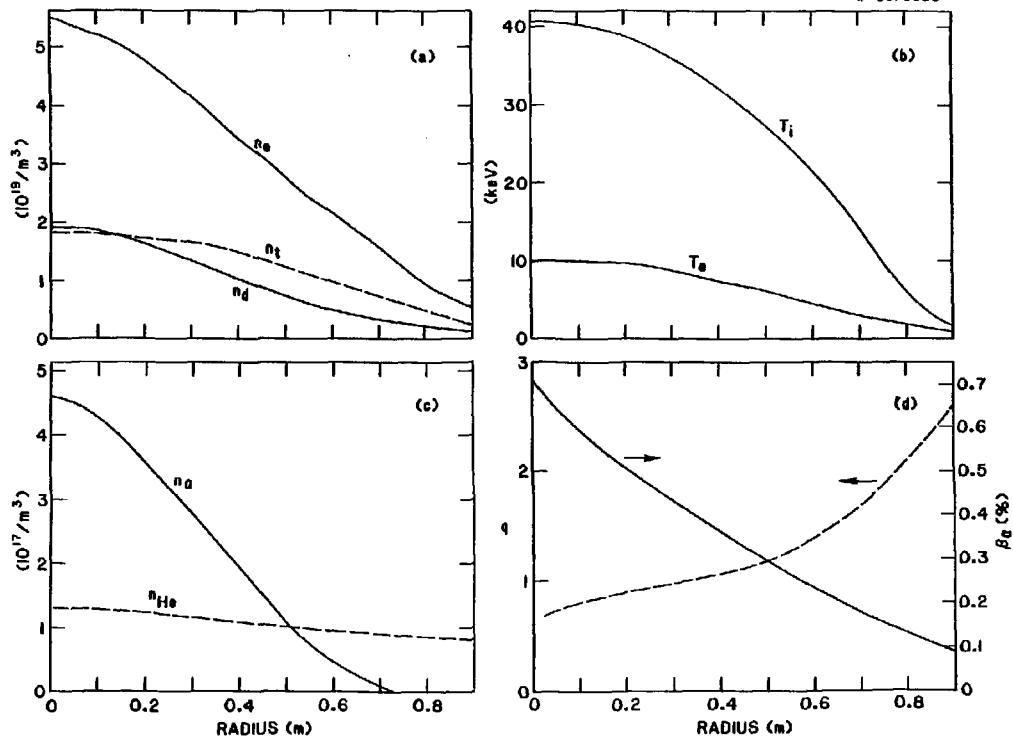


Fig. 5

EXTERNAL DISTRIBUTION IN ADDITION TO UC-20

Dr. Frank J. Paoloni, Univ of Wollongong, AUSTRALIA
 Prof. M.H. Brennan, Univ Sydney, AUSTRALIA
 Plasma Research Lab., Australian Nat. Univ., AUSTRALIA
 Prof. I.R. Jones, Flinders Univ., AUSTRALIA
 Prof. F. Cap, Inst Theo Phys, AUSTRIA
 Prof. M. Heindler, Institut für Theoretische Physik, AUSTRIA
 M. Goossens, Astronomisch Instituut, BELGIUM
 Ecole Royale Militaire, Lab de Phys Plasmas, BELGIUM
 Commission-European, Dg-XII Fusion Prog, BELGIUM
 Prof. R. Boucique, Laboratorium voor Natuurkunde, BELGIUM
 Dr. P.H. Sakanaka, Instituto Fisica, BRAZIL
 Instituto De Pesquisas Espaciais-INPE, BRAZIL
 Documents Office, Atomic Energy of Canada Limited, CANADA
 Dr. M.P. Bachynski, MPB Technologies, Inc., CANADA
 Dr. H.M. Skarsgard, University of Saskatchewan, CANADA
 Dr. H. Barnard, University of British Columbia, CANADA
 Prof. J. Teichmann, Univ. of Montreal, CANADA
 Prof. S.R. Sreenivasan, University of Calgary, CANADA
 Prof. Tudor W. Johnston, INRS-Energie, CANADA
 Dr. C.R. James, Univ. of Alberta, CANADA
 Dr. Peter Lukac, Komenskeho Univ, CZECHOSLOVAKIA
 The Librarian, Culham Laboratory, ENGLAND
 The Librarian, Rutherford Appleton Laboratory, ENGLAND
 Mrs. S.A. Hutchinson, JET Library, ENGLAND
 C. Mouttet, Lab. de Physique des Milieux Ionises, FRANCE
 J. Radet, CEN/CADARACHE - Bat 506, FRANCE
 Univ. of Ioannina, Library of Physics Dept. GREECE
 Dr. Tom Mui, Academy Bibliographic Ser., HONG KONG
 Preprint Library, Hungarian Academy of Sciences, HUNGARY
 Dr. B. Dasgupta, Saha Inst of Nucl. Phys., INDIA
 Dr. P. Kaw, Institute for Plasma Research, INDIA
 Dr. Philip Rosenau, Israel Inst. Tech, ISRAEL
 Librarian, Int'l Ctr Theo Phys, ITALY
 Prof. G. Rostagni, Univ Di Padova, ITALY
 Miss Clelia De Palo, Assoc EURATOM-ENEA, ITALY
 Biblioteca, Instituto di Fisica del Plasma, ITALY
 Dr. H. Yamato, Toshiba Res & Dev, JAPAN
 Prof. I. Kawakami, Atomic Energy Res. Institute, JAPAN
 Prof. Kyoji Nishikawa, Univ of Hiroshima, JAPAN
 Direc. Dept. Large Tokamak Res. JAERI, JAPAN
 Prof. Satoshi Itoh, Kyushu University, JAPAN
 Research Info Center, Nagoya University, JAPAN
 Prof. S. Tanaka, Kyoto University, JAPAN
 Library, Kyoto University, JAPAN
 Prof. Nobuyuki Inoue, University of Tokyo, JAPAN
 S. Nori, JAERI, JAPAN
 Librarian, Korea Advanced Energy Res. Institute, KOREA
 Prof. D.I. Choi, Adv. Inst Sci & Tech, KOREA
 Prof. B.S. Liley, University of Waikato, NEW ZEALAND
 Institute of Plasma Physics, PEOPLE'S REPUBLIC OF CHINA
 Librarian, Institute of Phys., PEOPLE'S REPUBLIC OF CHINA
 Library, Tsing Hua University, PEOPLE'S REPUBLIC OF CHINA
 Z. Li, Southwest Inst. Physics, PEOPLE'S REPUBLIC OF CHINA
 Prof. J.A.C. Cabral, Inst Superior Tecnico, PORTUGAL
 Dr. Octavian Petrus, AL I CUZA University, ROMANIA
 Dr. Johan de Villiers, Fusion Studies, AEC, SO AFRICA
 Prof. M.A. Hellberg, University of Natal, SO AFRICA
 C.I.E.M.A.T., Fusion Div. Library, SPAIN
 Dr. Lennart Stenflo, University of UMEA, SWEDEN
 Library, Royal Inst Tech, SWEDEN
 Prof. Hans Wilhelmson, Chalmers Univ Tech, SWEDEN
 Centre Phys des Plasmas, Ecole Polytech Fed, SWITZERLAND
 Bibliotheek, Fom-Inst Voor Plasma-Fysica, THE NETHERLANDS
 Dr. D.D. Ryutov, Siberian Acad Sci, USSR
 Dr. G.A. Eliseev, Kurchatov Institute, USSR
 Dr. V.A. Glukhikh, Inst Electrophysical Apparatus, USSR
 Dr. V.T. Tolok, Inst. Phys. Tech, USSR
 Dr. L.M. Kovrizhnykh, Institute Gen. Physics, USSR
 Nuclear Res. Establishment, Julich Ltd., W. GERMANY
 Bibliothek, Inst. Fur Plasmaforschung, W. GERMANY
 Dr. K. Schindler, Ruhr Universitat Bochum, W. GERMANY
 ASDEX Reading Rm, IPP/Max-Planck-Institut für
 Plasmaphysik, W. GERMANY
 Librarian, Max-Planck Institut, W. GERMANY
 Prof. R.K. Janev, Inst Phys, YUGOSLAVIA